

RESOLVING THE NEAR-FIELD FLOW PATTERNS OF AN IDEALIZED FIRE SPRINKLER WITH VOF MODELING AND ADAPTIVE MESH REFINEMENT

KARL V. MEREDITH¹, VUKO VUKČEVIĆ²

¹*Research Division, FM Global, Norwood MA, U.S.A., karl.meredith@fmglobal.com*

²*Univ. of Zagreb, Faculty of Mech. Engineering and Naval Architecture, Ivana Lučića 5, Zagreb, Croatia, v.vukcevic@wikki.co.uk*

Keywords: Fire suppression, primary atomization, volume of fluid, adaptive mesh refinement

The atomization of water by a fire sprinkler is of great interest to fire suppression research. The resulting droplet velocity, diameter, and liquid volume flux largely determine the suppression effectiveness. For example, large droplets can easily penetrate through a fire plume, while small droplets tend to be easily evaporated or carried away with the fire plume and have difficulty reaching the burning surfaces.

The goal of this work is to demonstrate the feasibility of using VOF modeling to adequately capture key aspects of sprinkler atomization in an idealized sprinkler geometry. Numerical modeling has been applied to understand the atomization behavior of an idealized sprinkler geometry consisting of a 9.5 mm inner-diameter cylindrical nozzle and a flat, 25.4 mm diameter disk with a liquid flow rate of 0.71 L/s. The simulations have been performed with *foam-extend-4.1* (a community driven fork of the OpenFOAM CFD software), using the ghost-fluid scheme and the isoAdvector scheme for interfacial reconstruction. In order to achieve efficient computations, a newly implemented adaptive-mesh-refinement (AMR) scheme has been used. Comparisons of atomization behavior (e.g. sheet-breakup length) and computational efficiency are made with previously measured results [1] and previous calculations [2] using static meshes. This study shows that using AMR coupled with VOF modeling can adequately obtain injection patterns in the near-field, and provides a path to subsequently simulate realistic sprinkler geometries.

Technical Approach

Numerical Model

The sprinkler simulations utilized a VOF solver, *navalFoam*, implemented in *foam-extend-4.1* [3], a community driven fork of the OpenFOAM [4] CFD software. The equations solved in *navalFoam* have been adequately documented elsewhere [5, 6], and portions of the model are reproduced here for reference purposes only. Equations (1-3) represent the continuity, momentum, and phase volume fraction transport equations, respectively,

$$\nabla \cdot \mathbf{U} = 0 \quad (1)$$

$$\frac{\partial(\mathbf{U})}{\partial t} + \nabla \cdot (\mathbf{U}\mathbf{U}) - \nabla \cdot (v_{eff} \nabla \mathbf{U}) = -\frac{\nabla p_d}{\rho} + \nabla \mathbf{U} \cdot \nabla v_{eff} \quad (2)$$

$$\frac{\partial \alpha}{\partial t} + \nabla \cdot (\mathbf{U}\alpha) = 0 \quad (3)$$

where \mathbf{U} represents the velocity vector, α represents the phase fraction, ρ is the density (assumes a combination of phase densities weighted by respective phase fractions), and v_{eff} is the effective kinematic viscosity from turbulence modeling. The phase fraction, α , will only have values between 0 and 1 over the few cells spanning the interface between fluids. The r.h.s. of Equation 2 represents the pressure body force and the variation of dynamic viscosity across the interface. The dynamic pressure is represented as

$$p_d = p - \rho \mathbf{g} \cdot \mathbf{x} \quad (4)$$

where \mathbf{g} is the gravity vector and \mathbf{x} represents the position vector. The pressure gradient discontinuity and surface tension are included within the discretization using the ghost fluid method (GFM) [6].





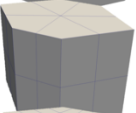
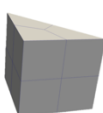


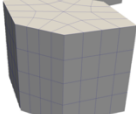
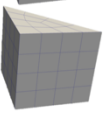


Rather than using typical interface compression schemes [18] to try to maintain a sharp interface, *navalFoam* includes the isoAdvector scheme [5] for approximating a geometric reconstruction of the interface. This scheme explicitly reconstructs a phase interface in each computational cell where $0 < \alpha < 1$ (i.e., at the intersection between the two phases). This interface is then advected through the cell at each time step. When calculating fluxes through cell faces, the interface information is used to determine the relative amounts of phase 1 or phase 2 to be advected out of the cell. This approach results in the ability to strongly limit numerical diffusion of the interface. A detailed description of the isoAdvector scheme is beyond the scope of this work, but additional details can be found in Ref. [5].

Large eddy simulation (LES) was used to treat turbulence, and the one-equation eddy model was used for simulating the turbulent kinetic energy. Additional details of the *navalFoam* model can be found in Refs. [6].

Adaptive Mesh Refinement

The recently implemented adaptive mesh refinement (AMR) scheme in *navalFoam* handles arbitrary polyhedra. The AMR algorithm operates by first identifying candidate cells for refinement. Through a composite process, multiple mesh refinement criteria can be used to precisely focus the candidate pool. For example, the mesh refinement criteria could be comprised of two conditions: 1) a minimum cell size (i.e., cube root of the cell volume), 2) a threshold for a scalar value (e.g. α), and a maximum refinement level. The user specifies the desired frequency (in terms of time steps) at which to perform the mesh refinement and unrefinement steps. These need not be the same frequency. Once the candidate pool is selected for refinement, the cells are then refined. Refinement proceeds by selecting the cell edges, splitting them, and creating a new node. A node is also placed at the centroid of each face, and at the centroid of the cell. New edges are then constructed to link the nodes together, forming the refined cells. Examples of this procedure for the various cell types are shown in Table 1. Unrefinement proceeds in reverse fashion.

Table 1: Polyhedral cell types covered by AMR implementation.

	Arbitrary	Prism	Pyramid	Tetrahedral
Original				
1 st refinement				
2 nd refinement				

Simulated Geometry

The simulated geometry, shown in Figure 1, consists of a cylindrical nozzle, $r = 4.25 \text{ mm}$ and $l = 28 \text{ mm}$, where r is the inner radius and l is the length. The pipe flow inside the nozzle is simulated, having the nozzle inlet at the top of the domain. A disk with diameter $d = 12.7 \text{ mm}$ is placed 20 mm below the nozzle outlet. The disk thickness is set to 2 mm. The overall domain bounds are $x = [-30 \text{ mm}, 30 \text{ mm}]$, $y = [-30 \text{ mm}, 30 \text{ mm}]$, and $z = [-30 \text{ mm}, 48 \text{ mm}]$. The top, bottom, and sides of the domain are open.

The inlet velocity was held constant at 10 m/s, which is a flow rate of 0.71 L/s (corresponding to a pressure of 0.55 bar) entering the nozzle inlet. This is near the upper range of flow rates tested in Ref. [14]. The inlet was set to a phase fraction of one, and represents the only source of water inflow into the domain. The nozzle and disk wall boundaries consisted of a no-slip velocity condition. The initial conditions were stationary with a zero liquid volume fraction. For this study, no turbulent fluctuations were specified at the inlet boundary. This assumption warrants further investigation in future studies, as an operating sprinkler will likely have large fluctuations at the inlet due to pump frequencies, turbulent pipe flow, and flow turning effects from the feed line (typically oriented perpendicular to the nozzle).

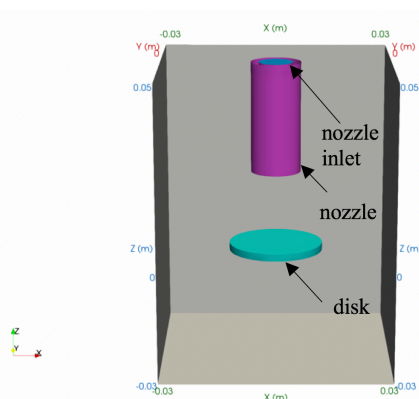


Figure 1: Simulated geometry showing the cylindrical nozzle oriented above the cylindrical disk with nozzle inlet, top, side, and bottom external boundaries shown.

Results and Discussion

The simulations were performed starting from a base mesh. The background mesh was 8 mm, and the finest mesh cells near the nozzle and the disk were $\sim 1 \text{ mm}$, yielding approximately 40K cells. A portion of the base mesh is shown in Figure 2 as a triangulated slice on the x-z plane.

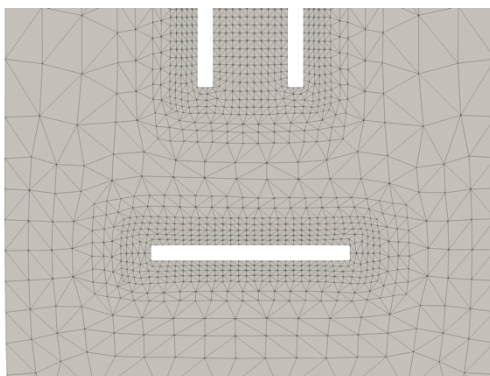


Figure 2: Base mesh for starting AMR simulations.

Five AMR criteria were simulated relating to minimum cell sizes of 1, 0.8, 0.6, 0.4, and 0.2 mm. In a previous study [2] using static meshes, it was shown that a mesh requirement of 0.5 mm and less is required to accurately predict the liquid film remaining in-tact in the vicinity of the deflector. The magnitude of the gradient of the phase fraction (α) was used as the refinement criterion, i.e., ($\text{mag}(\nabla\alpha)$). A value of 100 was selected for this criterion. Any cells with a gradient magnitude greater than 100, with a cell volume greater than the minimum cell size, and a refinement level less than the maximum refinement level specified (10), were selected for refinement.

An example of the mesh refinement for the 0.4 mm case is shown in Figure 3 at a simulated time of 10 ms. Refinement can be observed at the interface between the liquid and gas. Figure 3-b shows the magnitude of the gradient of liquid phase fraction, which accurately captures the interface between liquid and gas. Refinement based on the gradient of α leads to a sharp interface.

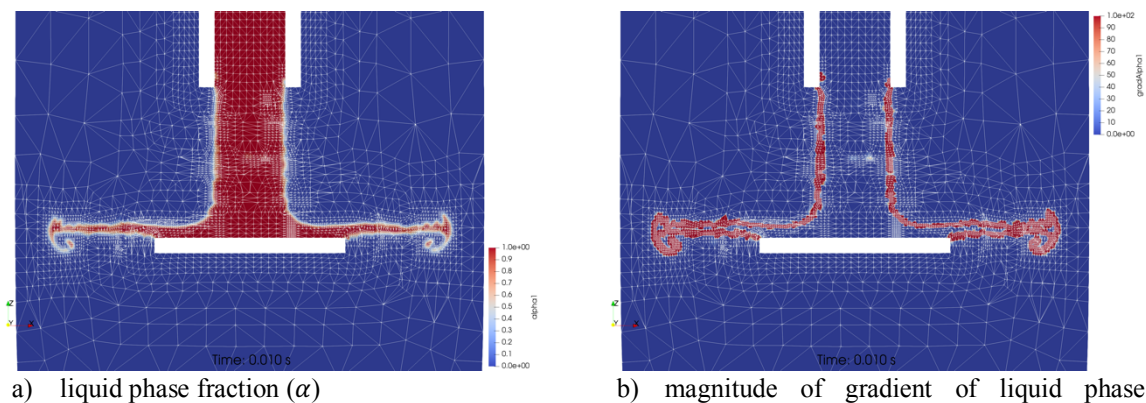


Figure 3: Liquid phase fraction and gradient used for grid refinement criterion shown for 0.4 mm case.

Near steady-state profiles for the various AMR cases are shown in Figure 4. The 1.0 mm mesh resolution clearly shows the liquid film breaking up within a few millimetres of the disk edge. The 0.6 mm mesh also shows, although difficult to make out from the figure, that the film breaks up along the edges of the film in the corners of the domain. The 0.4 mm mesh remains wholly intact. This behaviour matches previous static-mesh simulations [2], where the threshold for accurately predicting the sheet breakup distance (~ 160 mm for this case) was established for mesh resolutions of 0.5 mm and below. The 0.2 mm results, while only simulated out to 10 ms, are expected to yield similar results to the 0.4 mm mesh.

Summary and Conclusions

Simulating the atomization processes of a sprinkler has the potential to allow for enhanced insight into the key physics and controlling parameters. This approach also has the potential to be used as a predictive tool to estimate the spray injection profiles. In this study, the atomization of an idealized sprinkler geometry was simulated, and comparisons were made to experimental observations. The feasibility of using an adaptive mesh refinement scheme to reproduce flow features in the near-field region was demonstrated. Additionally, an innovative isoAdvector scheme allowed for maintaining a sharp interface even with relatively coarse mesh resolution. Computational cost of each simulation was quantified.

Similar to the previous static-mesh study, the AMR study revealed that mesh resolutions of 1.0, 0.8, and 0.6 mm provided insufficient refinement, as the sheet breakup distance was greatly under predicted due to numerical diffusion of the interface. Mesh resolutions of 0.4 and 0.2 mm yield results consistent with experimental observations. Ultimately, a mesh resolution of less than 0.2 mm or less will be required to resolve the flow features necessary to accurately predict atomization processes due to the anticipated drop size. Comparisons for film thickness predictions were also made, showing the simulated values fall within the expected range.

This study establishes the feasibility of using VOF modeling with AMR to adequately obtain injection patterns in the near-field. The numerical model can subsequently be used to predict atomization at locations beyond sheet breakup. This

work has provided a foundation for eventually to simulating realistic sprinkler geometries to obtain the atomization results necessary to initialize the sprinkler spray in fire suppression simulations.

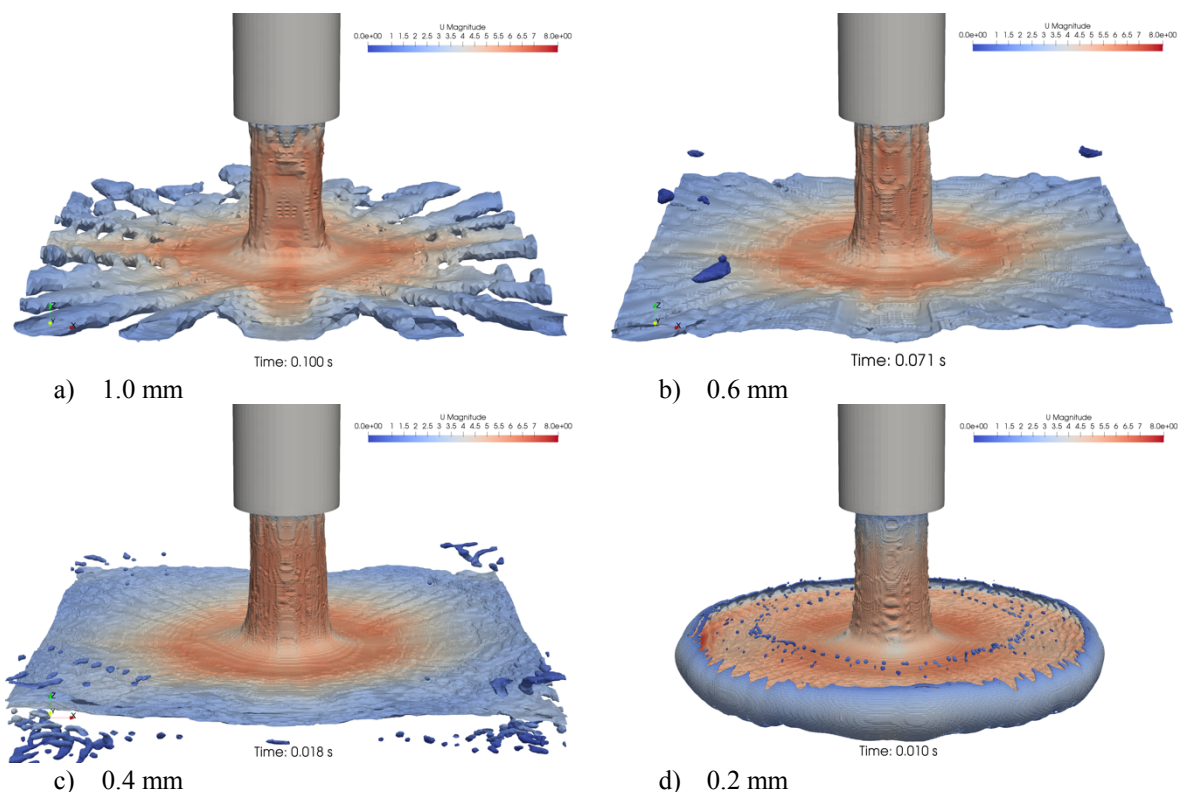


Figure 4: Isocontours of $\alpha=0.5$ colored by velocity magnitude [m/s] for various minimum cell size criteria.

Acknowledgements

This work was funded by FM Global as part of the Strategic Research Program for Fire and Suppression Modeling. Dr. Hrv Jasak of Wikki Ltd. is gratefully acknowledged for developing *navalFoam* and for providing guidance on the use of it.

References

- [1] Zhou, X. and H.-Z. Yu, *Experimental investigation of spray formation as affected by sprinkler geometry*. Fire Safety Journal, 2011. **46**: p. 140-150.
- [2] Meredith, K.V., X. Zhou, and Y. Wang, *Towards Resolving the Atomization Process of an Idealized Fire Sprinkler with VOF Modeling*, in *ILAS-Europe 2017, 28th Conference on Liquid Atomization and Spray Systems*. 2017: Valencia, Spain.
- [3] *foam-extend*. 2016 [cited 2017 June 13]; Available from: <http://www.sourceforge.net/projects/foam-extend>.
- [4] Weller, H.G., et al., *A tensorial approach to computational continuum mechanics using object-oriented techniques*. Computers in Physics, 1998. **12**(6): p. 620-631.
- [5] Roenby, J., H. Bredmose, and H. Jasak, *A computational method for sharp interface advection*. Royal Society Publishing open sci, 2016. **3**(160405).
- [6] Vukcevic, V., H. Jasaka, and I. Gatina, *Implementation of the Ghost Fluid Method for free surface flows in polyhedral Finite Volume framework*. Computers and Fluids, 2017. **153**: p. 1-19.